

The twisted bilayer: an experimental and theoretical review

J.M.B. Lopes dos Santos

CFP e Departamento de Física, Faculdade de Ciências, Universidade do Porto

Graphene, 2009 – Benasque



- 1 Moiré in Graphite and FLG
- 2 Continuum theory
- 3 Results
- 4 Experimental and theoretical confirmation
- 5 Magnetic Field

Outline

- 1 Moiré in Graphite and FLG
- 2 Continuum theory
- 3 Results
- 4 Experimental and theoretical confirmation
- 5 Magnetic Field

Moiré in graphite and FLG

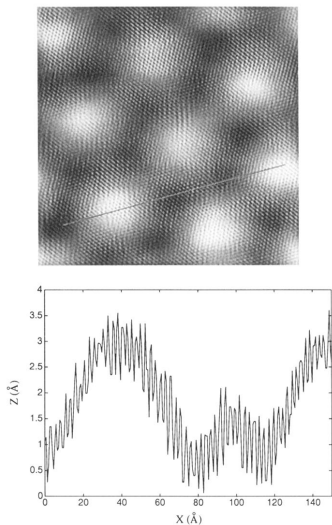
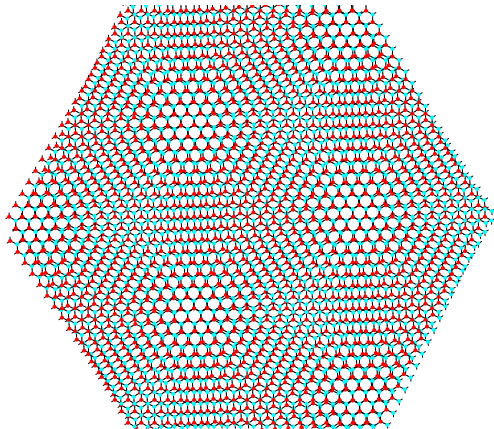


FIG. 2. (a) A closeup view of the superlattice on which graphite atoms are resolved. The image is taken with set current 5.6 nA, tip bias 72 mV, and scan size $202 \times 202 \text{ \AA}^2$. The image is low pass filtered. (b) A cross section along the direction indicated by the line in (a).

$$L = \frac{a_0}{2 \sin(\theta/2)} \approx \frac{a_0}{\theta}$$



Moiré in graphite and FLG

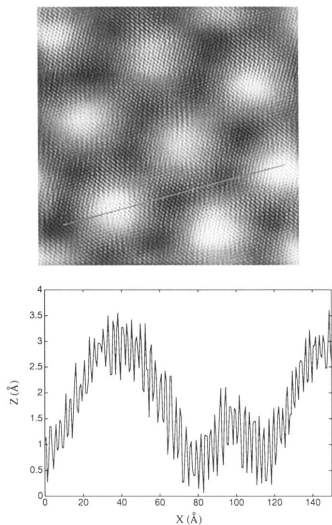
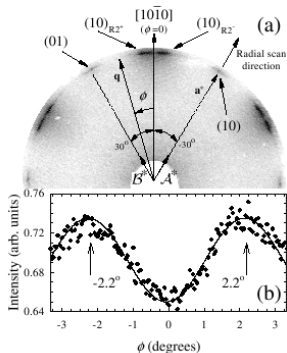


FIG. 2. (a) A closeup view of the superlattice on which graphite atoms are resolved. The image is taken with set current 5.6 nA, tip bias 72 mV, and scan size $202 \times 202 \text{ \AA}^2$. The image is low pass filtered. (b) A cross section along the direction indicated by the line in (a).

$$L = \frac{a_0}{2 \sin(\theta/2)} \approx \frac{a_0}{\theta}$$



J. Hass, *et. al* PRL (2008)

Latil *et al.* PRB (2007)

Rong and Kuiper, PRB 1993

Moiré in graphite and FLG

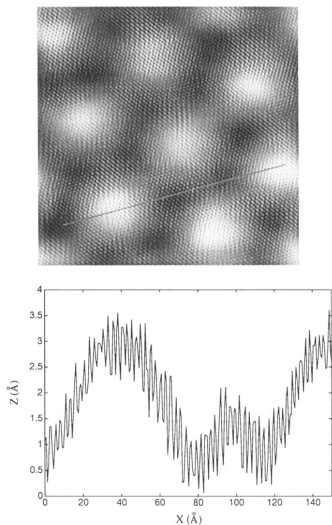
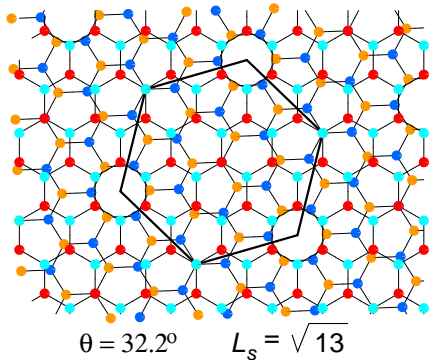


FIG. 2. (a) A closeup view of the superlattice on which graphite atoms are resolved. The image is taken with set current 5.6 nA, tip bias 72 mV, and scan size $202 \times 202 \text{ \AA}^2$. The image is low pass filtered. (b) A cross section along the direction indicated by the line in (a).

$$L = \frac{a_0}{2 \sin(\theta/2)} \approx \frac{a_0}{\theta}$$



Moiré in graphite and FLG

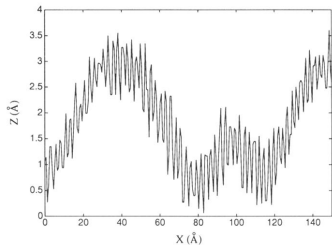
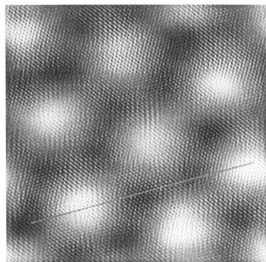
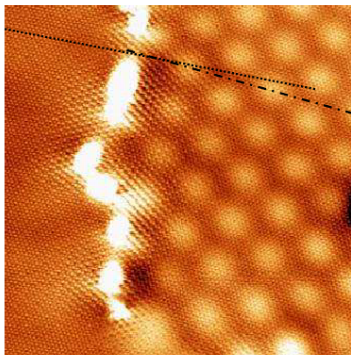


FIG. 2. (a) A closeup view of the superlattice on which graphite atoms are resolved. The image is taken with set current 5.6 nA, tip bias 72 mV, and scan size $202 \times 202 \text{ \AA}^2$. The image is low pass filtered. (b) A cross section along the direction indicated by the line in (a).

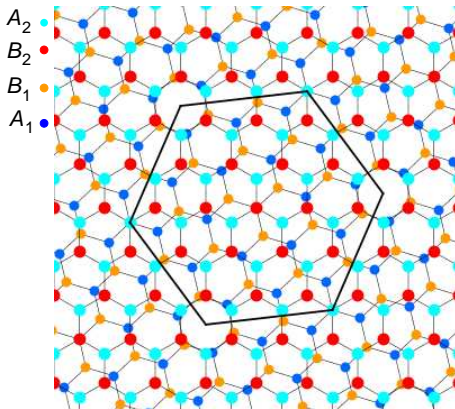
$$L = \frac{a_0}{2 \sin(\theta/2)} \approx \frac{a_0}{\theta}$$



Varchon *et. al*, PRB (2008)

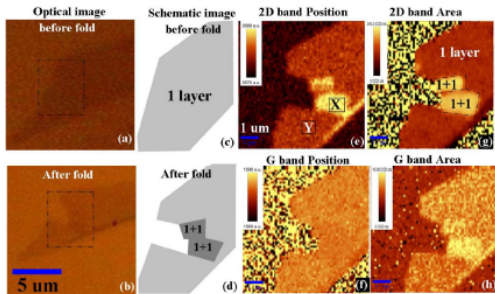
Rong and Kuiper, PRB 1993

Controversy

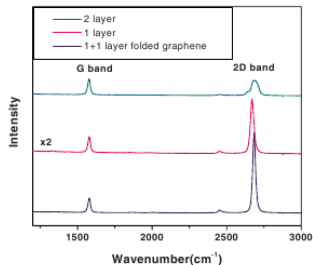


Bilayer	Graphite	Xhie et. al (PRB, 93)	Rong Kuiper (PRB,93)
BA(Ah)	BAB(AhA)	Bright ($M - \beta$)	Gray
AA (BB)	AAB (BBh)	Dark ($M - h$)	Bright
AB(Bh)	ABh(BhA)	Gray ($M - \alpha$)	Dark

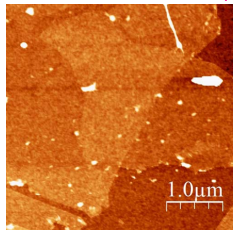
Moire in Exfoliated Graphene



REDUCTION OF FERMI VELOCITY IN FOLDED...

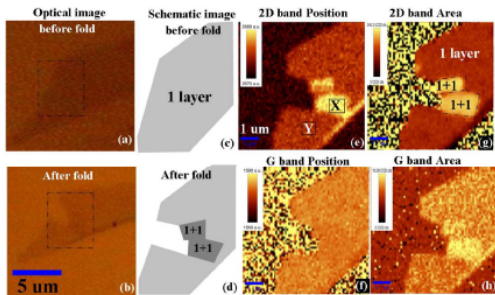


Zenhua Ni *et al*, PRB (2008)

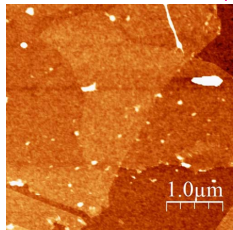


Poncharal *et al*, PRB (2008)

Moire in Exfoliated Graphene

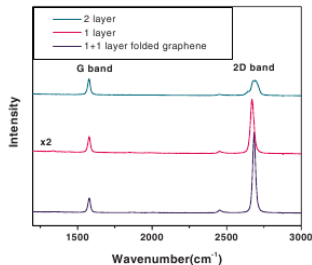


Zenhua Ni *et al*, PRB (2008)



Poncharal *et al*, PRB (2008)

REDUCTION OF FERMI VELOCITY IN FOLDED...



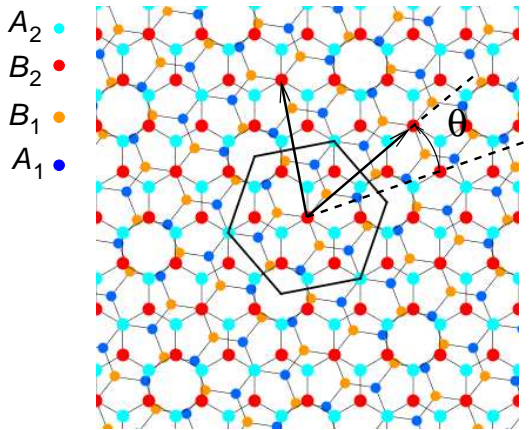
Raman 2D band looks like SLG, not like the bilayer, but blue shifted.

Outline

- 1 Moiré in Graphite and FLG
- 2 Continuum theory**
- 3 Results
- 4 Experimental and theoretical confirmation
- 5 Magnetic Field

Commensurability

LdS, Peres, Castro Neto, PRL, 2007



$$\cos(\theta_i) = \frac{3i^2 + 3i + 1/2}{3i^2 + 3i + 1}$$

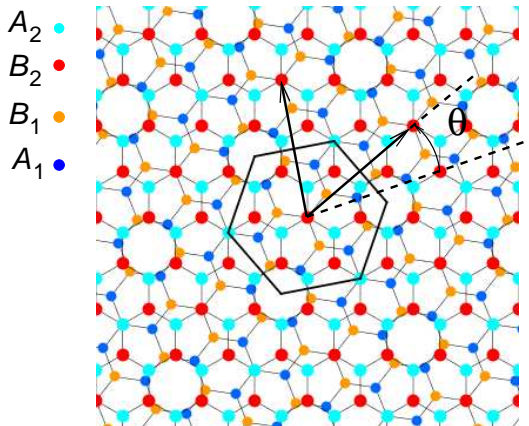
$$\mathbf{t}_1 = i\mathbf{a}_1 + (i + 1)\mathbf{a}_2$$

$$\mathbf{t}_2 = -(i + 1)\mathbf{a}_1 + (2i + 1)\mathbf{a}_2$$

$$i = 1 \Rightarrow \theta = 21.8^\circ, \quad L = 8 \text{ \AA}$$

Commensurability

LdS, Peres, Castro Neto, PRL, 2007



$$\cos(\theta_i) = \frac{3i^2 + 3i + 1/2}{3i^2 + 3i + 1}$$

$$\mathbf{t}_1 = i\mathbf{a}_1 + (i+1)\mathbf{a}_2$$

$$\mathbf{t}_2 = -(i+1)\mathbf{a}_1 + (2i+1)\mathbf{a}_2$$

$$i = 1 \Rightarrow \theta = 21.8^\circ, \quad L = 8 \text{ \AA}$$

Other angles are possible

Shallcross, PRL 2008.

Continuum limit ($k \cdot p$ approximation)

- Layer 1

$$\mathcal{H}_1 = -t \sum_i a_1^\dagger(\mathbf{r}_i) [b_1(\mathbf{r}_i + \delta_1) + b_1(\mathbf{r}_i + \delta_2) + b_1(\mathbf{r}_i + \delta_3)] + hc$$

$$a_1(\mathbf{r}) \rightarrow v_c^{1/2} \psi_a(\mathbf{r}) \exp(i\mathbf{K} \cdot \mathbf{r}) + \dots$$

$$b_1(\mathbf{r}) \rightarrow v_c^{1/2} \psi_b(\mathbf{r}) \exp(i\mathbf{K} \cdot \mathbf{r}) + \dots$$

$$\hbar v_F \sum_k \psi'^{\dagger}(\mathbf{r}) \begin{bmatrix} 0 & -i\partial_x - \partial_y \\ -i\partial_x + \partial_y & 0 \end{bmatrix} \psi'(\mathbf{r}).$$

Continuum limit ($k \cdot p$ approximation)

- layer 2 (rotated)

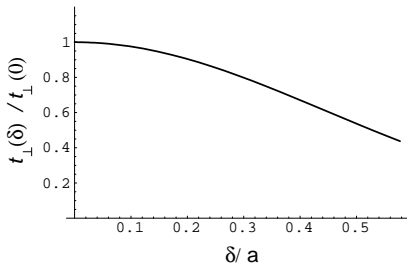
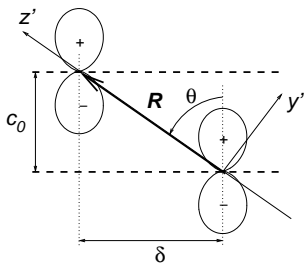
$$\mathcal{H}_2 = -t \sum_j b_2^\dagger(\mathbf{r}_j) [a_2(\mathbf{r}_j + \mathbf{s}'_0) + a_2(\mathbf{r}_j + \mathbf{s}'_0 - \mathbf{a}'_1) + a_2(\mathbf{r}_j + \mathbf{s}'_0 - \mathbf{a}'_2)] + hc$$

$$a_2(\mathbf{r}) \rightarrow v_c^{1/2} \psi_{a'}(\mathbf{r}) \exp(i\mathbf{K}^\theta \cdot \mathbf{r}) + \dots$$

$$b_2(\mathbf{r}) \rightarrow v_c^{1/2} \psi_{b'}(\mathbf{r}) \exp(i\mathbf{K}^\theta \cdot \mathbf{r}) + \dots$$

$$\hbar v_F \sum_k \psi'^{\dagger}(\mathbf{r}) \begin{bmatrix} 0 & e^{i\theta} (-i\partial_x - \partial_y) \\ e^{-i\theta} (-i\partial_x + \partial_y) & 0 \end{bmatrix} \psi'(\mathbf{r}).$$

Parametrization of $t_{\perp}(\mathbf{r})$



$$t_{\perp}(\delta) = V_{pp\sigma}(d) \cos^2 \theta + V_{pp\pi}(d) \sin^2 \theta \propto t_{\perp}$$

Tang, et al Phys. Rev B 53,979 (1996)

Inter-layer hopping

- Electrons hop from atom in layer 1 to closest atom—of either sub-lattice— in layer 2;

$$\mathbf{r}'(\mathbf{r}) = \mathbf{r} + \delta(\mathbf{r}) \quad (\text{plane coordinates})$$

$$t_{\perp} \rightarrow t_{\perp}[\delta^{\beta\alpha}(\mathbf{r})] \equiv t_{\perp}^{\beta\alpha}(\mathbf{r}) \quad \alpha(\beta) = A_1, B_1(A_2, B_2)$$

$$\mathcal{H}_{\perp} = \sum_{\alpha,\beta} \int d^2r t_{\perp}^{\beta\alpha}(\mathbf{r}) e^{i\mathbf{K}^{\theta} \cdot \delta_{\alpha\beta}(\mathbf{r})} e^{i\Delta\mathbf{K} \cdot \mathbf{r}} \psi_{1,\alpha}^{\dagger}(\mathbf{r}) \psi_{2,\beta}(\mathbf{r}) + h.c.$$

- $t_{\perp}^{\beta\alpha}(\mathbf{r}) e^{i\mathbf{K}^{\theta} \cdot \delta_{\alpha\beta}(\mathbf{r})}$: period of Moiré pattern.
- $(\Delta\mathbf{K} = \mathbf{K}^{\theta} - \mathbf{K})$; $\mathbf{k} \rightarrow \mathbf{k} + \Delta\mathbf{K}/2$ layer 1 ; $\mathbf{k} \rightarrow \mathbf{k} - \Delta\mathbf{K}/2$ layer 2;

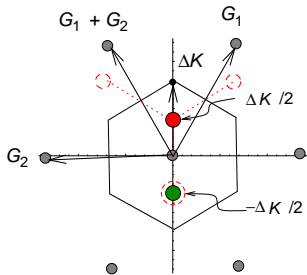
$$\mathcal{H}_\perp = \sum_{\alpha,\beta} \sum_{\mathbf{k},\mathbf{G}} \tilde{t}_\perp^{\beta\alpha}(\mathbf{G}) \phi_{\alpha,\mathbf{k}+\mathbf{G}}^\dagger \phi_{\beta',\mathbf{k}} + h.c.$$

$$\tilde{t}_\perp^{\alpha\beta}(\mathbf{G}) = \frac{1}{V_c} \int_{uc} d^2r t_\perp^{\alpha\beta}(\mathbf{r}) e^{i\mathbf{K}^\theta \cdot \delta_{AB}(\mathbf{r})} e^{-i\mathbf{G} \cdot \mathbf{r}}$$

- Dirac electrons with periodic interlayer coupling.

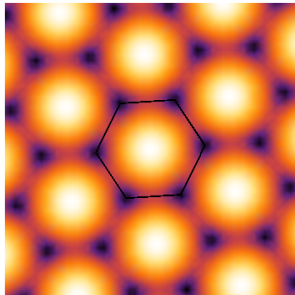
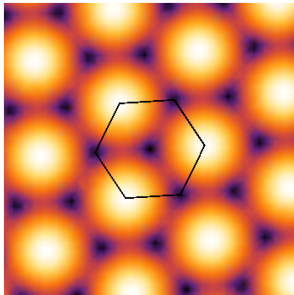
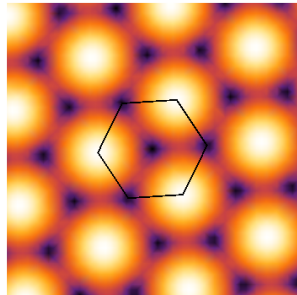
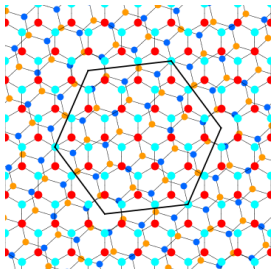
Results for $\tilde{t}_{\perp}^{\alpha\beta}(\mathbf{G})$

- Exact symmetries $\delta^{AB} \leftrightarrow \delta^{BA}$ e $\delta^{AA} \leftrightarrow \delta^{BB}$;
- limit $\theta \ll 1$, $\delta^{AA} \leftrightarrow \delta^{BA}$;



\mathbf{G}	0	$-\mathbf{G}_1$	$-\mathbf{G}_1 - \mathbf{G}_2$
$\tilde{t}_{\perp}^{BA}(\mathbf{G})$	\tilde{t}_{\perp}	\tilde{t}_{\perp}	\tilde{t}_{\perp}
$\tilde{t}_{\perp}^{AB}(\mathbf{G})$	\tilde{t}_{\perp}	$e^{-i2\pi/3}\tilde{t}_{\perp}$	$e^{i2\pi/3}\tilde{t}_{\perp}$
$\tilde{t}_{\perp}^{AA}(\mathbf{G})$	\tilde{t}_{\perp}	$e^{i2\pi/3}\tilde{t}_{\perp}$	$e^{-i2\pi/3}\tilde{t}_{\perp}$
$\tilde{t}_{\perp}^{BB}(\mathbf{G})$	\tilde{t}_{\perp}	$e^{i2\pi/3}\tilde{t}_{\perp}$	$e^{-i2\pi/3}\tilde{t}_{\perp}$

Real Space Coupling

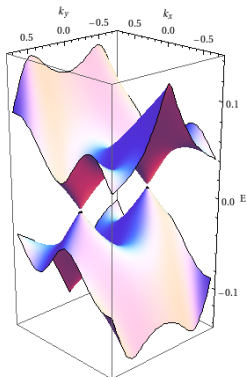
 \tilde{t}_{\perp}^{BA}  $\tilde{t}_{\perp}^{AA}, \tilde{t}_{\perp}^{BB}$  \tilde{t}_{\perp}^{AB} 

$$\tilde{t}_{\perp}^{\beta\alpha}(\mathbf{r}) = \sum_{\mathbf{G}} \tilde{t}_{\perp}^{\beta\alpha}(\mathbf{G}) e^{i\mathbf{G}\cdot\mathbf{r}} e^{i\Delta\mathbf{K}\cdot\mathbf{r}}$$

Outline

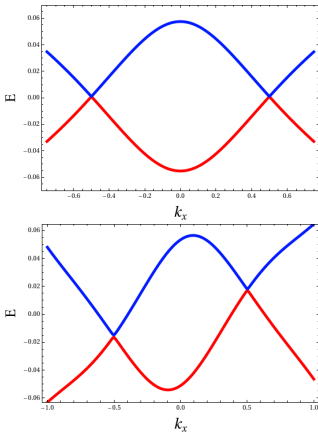
- 1 Moiré in Graphite and FLG
- 2 Continuum theory
- 3 Results**
- 4 Experimental and theoretical confirmation
- 5 Magnetic Field

Electronic Structure



Linear Dispersion relation at low energies. New energy scale, $\hbar v_F \Delta K \approx 0.19 \text{ eV} \times \theta^0$.

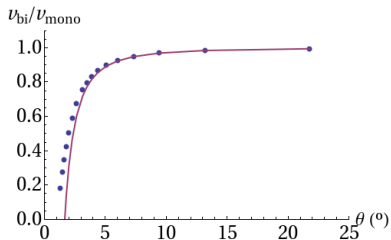
Electronic Structure



Linear Dispersion relation at low energies. New energy scale, $\hbar v_F \Delta K \approx 0.19 \text{ eV} \times \theta^0$.

Electric field bias does not open a gap.

Electronic Structure



$$\frac{v'_F}{v_F} \approx 1 - 9 \left(\frac{\tilde{t}_\perp}{\hbar v_F \Delta K} \right)^2$$

$$(\tilde{t}_\perp \ll \hbar v_F \Delta K)$$

Linear Dispersion relation at low energies. New energy scale, $\hbar v_F \Delta K \approx 0.19 \text{ eV} \times \theta^\circ$.

Electric field bias does not open a gap.

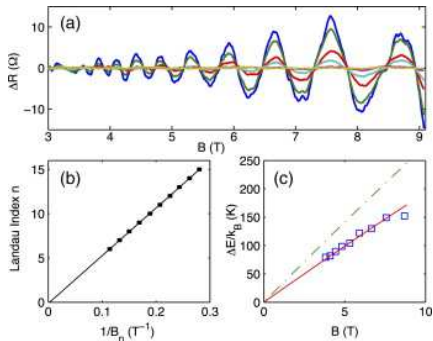
v_F is reduced relative to the single layer.

Outline

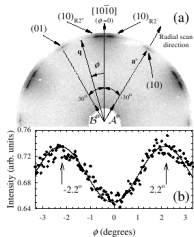
- 1 Moiré in Graphite and FLG
- 2 Continuum theory
- 3 Results
- 4 Experimental and theoretical confirmation**
- 5 Magnetic Field

Epitaxial graphene

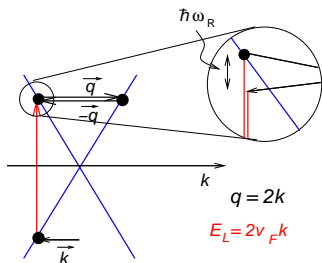
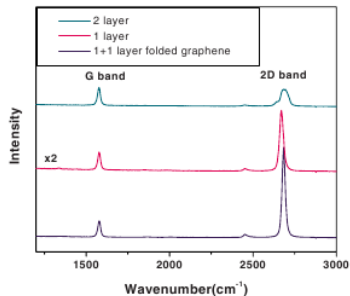
Epitaxial graphene often displays SLG behaviour.



de Heer et. al. *Sol. St. Comm.* vol 143, 92, (2007)



REDUCTION OF FERMI VELOCITY IN FOLDED...



Raman in Moire bilayers

$$\hbar\omega_R = 2E_{ph} \left(\frac{E_L}{v_f} \right)$$

$$\frac{v_F}{E_L} \delta\omega_R \propto -\frac{\delta v_F}{v_F}$$

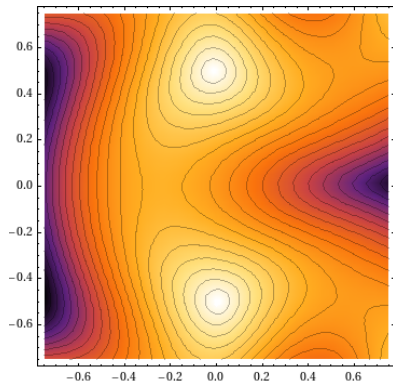
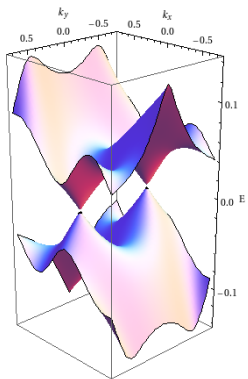
For a 5% reduction, $\theta \sim 7^\circ$,

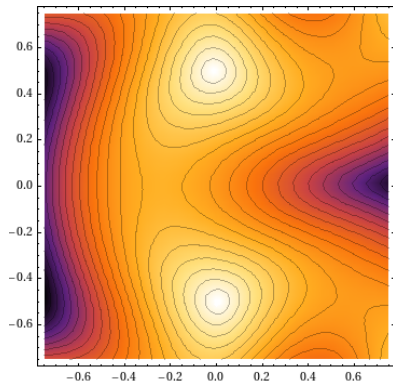
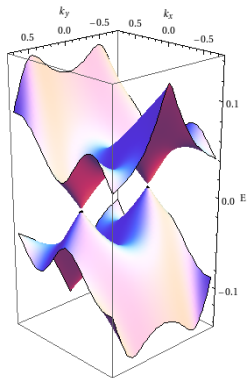
$\hbar v_F \Delta K \sim 1.4 \text{ eV}$,

$E_L = 2.33 \text{ eV}$.

Dependence of $\delta\omega_R$ with E_L seems wrong.

DOS by STS

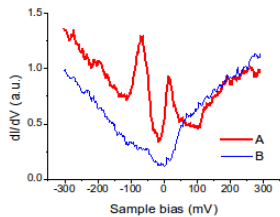
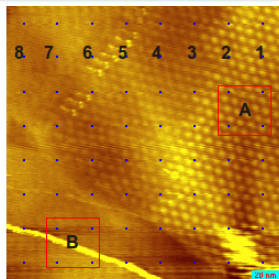




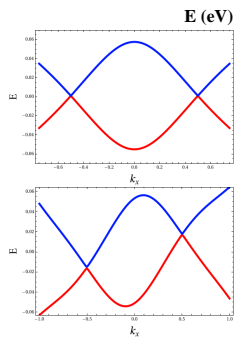
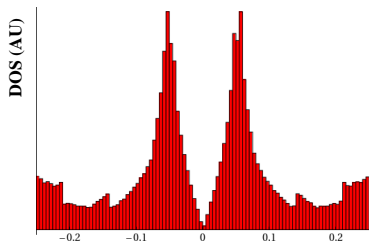
Low energy VHP

Low energy Van Hove peaks (saddle point) predicted at meeting of two cones.

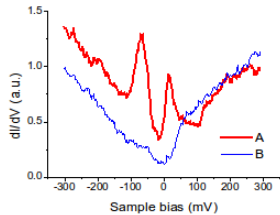
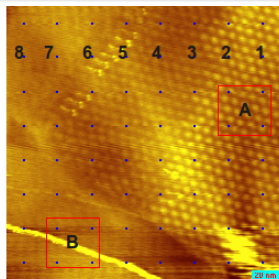
DOS by STS



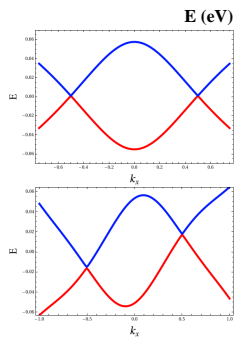
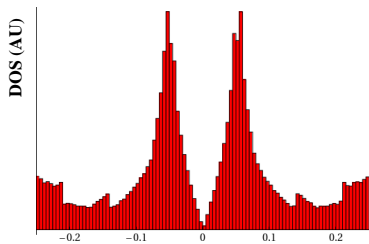
E. Andrei *et. al.* (unpublished)



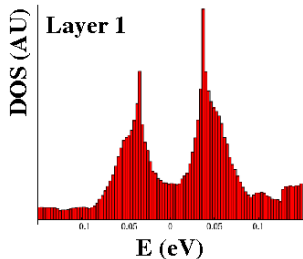
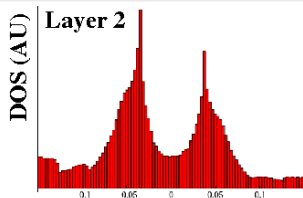
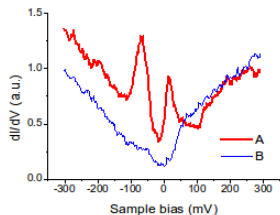
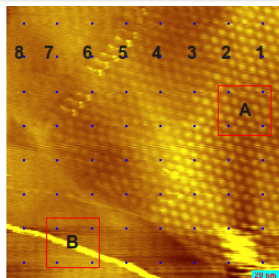
DOS by STS



E. Andrei *et. al.* (unpublished)



DOS by STS

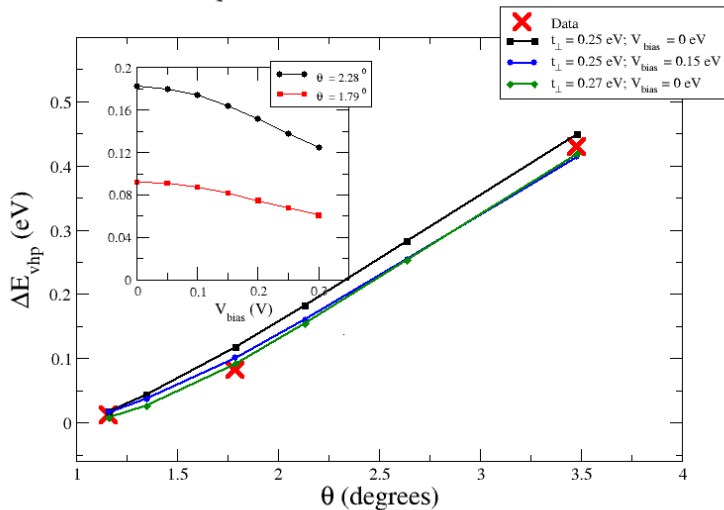


E. Andrei *et. al.* (unpublished)

Bias shifts cones \Rightarrow DOS does not vanish, and is different in the two layers.

Three data points!

Separation between Van-Hove Peaks



Outline

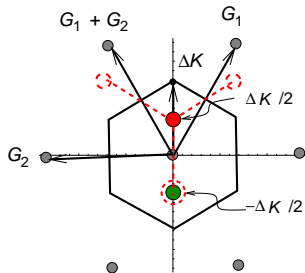
- 1 Moiré in Graphite and FLG
- 2 Continuum theory
- 3 Results
- 4 Experimental and theoretical confirmation
- 5 **Magnetic Field**

Modulated interlayer hopping

Two planes of Dirac massless fermions coupled by modulated hopping

$$\mathcal{H}_\perp = \int d^2r t_\perp^{\beta\alpha}(\mathbf{r}) e^{i\mathbf{K}^\theta \cdot \delta_{\beta\alpha}(\mathbf{r})} e^{i\Delta\mathbf{K} \cdot \mathbf{r}} \psi_{\alpha 1}^\dagger(\mathbf{r}) \psi_{\beta 2}(\mathbf{r}) + h.c.$$

- $t_\perp^{\beta\alpha}(\mathbf{r}) e^{i\mathbf{K}^\theta \cdot \delta_{\beta\alpha}(\mathbf{r})} \rightarrow$ period of superlattice: \mathbf{t}_1 , \mathbf{t}_2 ;
- $e^{i\Delta\mathbf{K} \cdot \mathbf{r}} \rightarrow$ period $3\times$ that of superlattice, $3\mathbf{t}_1$, $3\mathbf{t}_2$, because $\Delta\mathbf{K} = (\mathbf{g}_1 + 2\mathbf{g}_2)/3$.

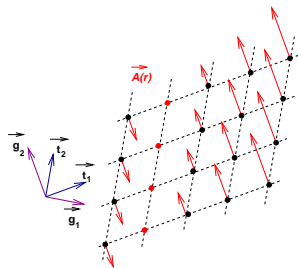


Funny gauge

$$\mathcal{H}_l^{(\mathbf{K})} = -tL_s^{-1} \times \begin{bmatrix} 0 & -ie^{-i\theta} \left(\mathbf{t}_1 e^{-i\frac{2\pi}{3}} + \mathbf{t}_2 e^{+i\frac{2\pi}{3}} \right) \cdot \left(\frac{\nabla}{i} - \frac{e}{\hbar c} \mathbf{A} \right) \\ ie^{i\theta} \left(\mathbf{t}_1 e^{i\frac{2\pi}{3}} + \mathbf{t}_2 e^{-i\frac{2\pi}{3}} \right) \cdot \left(\frac{\nabla}{i} - \frac{e}{\hbar c} \mathbf{A} \right) & 0 \end{bmatrix}$$

$$\mathbf{A} = (|\mathbf{t}_1 \times \mathbf{t}_2| B x_1 / 2\pi) \mathbf{g}_2$$

$$\mathcal{H}^{(\mathbf{K})} = -tL_s^{-1} \times \begin{bmatrix} 0 & \mathbf{D}^\dagger \\ \mathbf{D} & 0 \end{bmatrix}$$



$$\mathbf{r} = x_1 \mathbf{t}_1 + x_2 \mathbf{t}_2$$

$$\mathbf{D} = ie^{i\theta} \left[e^{i\frac{2\pi}{3}} \frac{\partial_1}{i} + e^{-i\frac{2\pi}{3}} \left(\frac{\partial_2}{i} - 2\pi \frac{\phi_s}{\phi_0} x_1 \right) \right]$$

Perturbation invariant under $(x_1, x_2) \rightarrow (x_1 + m, x_2 + n) \implies$ Bloch waves on x_2 .

Symmetry adapted basis

- $\Psi_{k_2, m}(x_1, x_2) = e^{ik_2 x_2} \mathbf{u}(x_1, x_2) = e^{ik_2 x_2} e^{i2\pi m x_2} \Phi(x_1).$

Symmetry adapted basis

- $\Psi_{k_2, m}(x_1, x_2) = e^{ik_2 x_2} \mathbf{u}(x_1, x_2) = e^{ik_2 x_2} e^{i2\pi m x_2} \Phi(x_1)$.
- $\partial_2 \rightarrow i(k_2 + 2\pi m) \Rightarrow \mathbf{D}, \mathbf{D}^\dagger \rightarrow a, a^\dagger$;

Symmetry adapted basis

- $\Psi_{k_2, m}(x_1, x_2) = e^{ik_2 x_2} \mathbf{u}(x_1, x_2) = e^{ik_2 x_2} e^{i2\pi m x_2} \Phi(x_1).$
- $\partial_2 \rightarrow i(k_2 + 2\pi m) \Rightarrow \mathbf{D}, \mathbf{D}^\dagger \rightarrow a, a^\dagger;$
- $\Psi'_{k_2, m, n}(x_1, x_2) = A e^{ik_2 x_2} e^{i2\pi m x_2} \begin{bmatrix} \phi_n(x_1 - \frac{k_2}{2\pi} \frac{\phi_0}{\phi_s} - m \frac{\phi_0}{\phi_s}) \\ \mp \phi_{n-1}(x_1 - \frac{k_2}{2\pi} \frac{\phi_0}{\phi_s} - m \frac{\phi_0}{\phi_s}) \end{bmatrix}$

Symmetry adapted basis

- $\Psi_{k_2, m}(x_1, x_2) = e^{ik_2 x_2} \mathbf{u}(x_1, x_2) = e^{ik_2 x_2} e^{i2\pi m x_2} \Phi(x_1).$

- $\partial_2 \rightarrow i(k_2 + 2\pi m) \Rightarrow \mathbf{D}, \mathbf{D}^\dagger \rightarrow a, a^\dagger;$

- $\Psi'_{k_2, m, n}(x_1, x_2) = A e^{ik_2 x_2} e^{i2\pi m x_2} \begin{bmatrix} \phi_n(x_1 - \frac{k_2}{2\pi} \frac{\phi_0}{\phi_s} - m \frac{\phi_0}{\phi_s}) \\ \mp \phi_{n-1}(x_1 - \frac{k_2}{2\pi} \frac{\phi_0}{\phi_s} - m \frac{\phi_0}{\phi_s}) \end{bmatrix}$

- k_2 is a good (Bloch) quantum number in presence of perturbation.

$$\tilde{t}_\perp^{\alpha\beta}(0) e^{i\Delta\mathbf{K}\cdot\mathbf{r}} + \tilde{t}_\perp^{\alpha\beta}(-\mathbf{G}_1) e^{i(\Delta\mathbf{K}-\mathbf{G}_1)\cdot\mathbf{r}} + \tilde{t}_\perp^{\alpha\beta}(-\mathbf{G}_1 - \mathbf{G}_2) e^{i(\Delta\mathbf{K}-\mathbf{G}_1-\mathbf{G}_2)\cdot\mathbf{r}}$$

Symmetry adapted basis

- $\Psi_{k_2, m}(x_1, x_2) = e^{ik_2 x_2} \mathbf{u}(x_1, x_2) = e^{ik_2 x_2} e^{i2\pi m x_2} \Phi(x_1).$

- $\partial_2 \rightarrow i(k_2 + 2\pi m) \Rightarrow \mathbf{D}, \mathbf{D}^\dagger \rightarrow a, a^\dagger;$

- $\Psi'_{k_2, m, n}(x_1, x_2) = A e^{ik_2 x_2} e^{i2\pi m x_2} \begin{bmatrix} \phi_n(x_1 - \frac{k_2}{2\pi} \frac{\phi_0}{\phi_s} - m \frac{\phi_0}{\phi_s}) \\ \mp \phi_{n-1}(x_1 - \frac{k_2}{2\pi} \frac{\phi_0}{\phi_s} - m \frac{\phi_0}{\phi_s}) \end{bmatrix}$

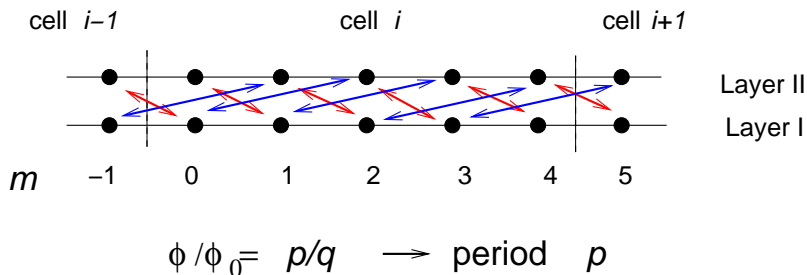
- k_2 is a good (Bloch) quantum number in presence of perturbation.

$$\tilde{t}_\perp^{\alpha\beta}(0) e^{i\Delta\mathbf{K}\cdot\mathbf{r}} + \tilde{t}_\perp^{\alpha\beta}(-\mathbf{G}_1) e^{i(\Delta\mathbf{K}-\mathbf{G}_1)\cdot\mathbf{r}} + \tilde{t}_\perp^{\alpha\beta}(-\mathbf{G}_1 - \mathbf{G}_2) e^{i(\Delta\mathbf{K}-\mathbf{G}_1-\mathbf{G}_2)\cdot\mathbf{r}}$$

- \mathbf{r} -dependence = $\exp(\alpha_1 2\pi x_1 + \alpha_2 2\pi x_2)$ $\alpha_1 = 2, -1; \alpha_2 = 1, -2$

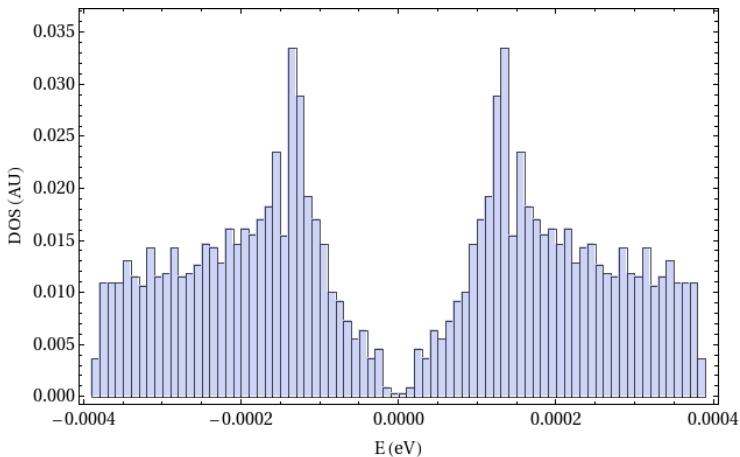
- x_1 terms \Rightarrow diagonal in m
- x_2 terms $\Rightarrow m \rightarrow m - \alpha_2$

Harper Problem



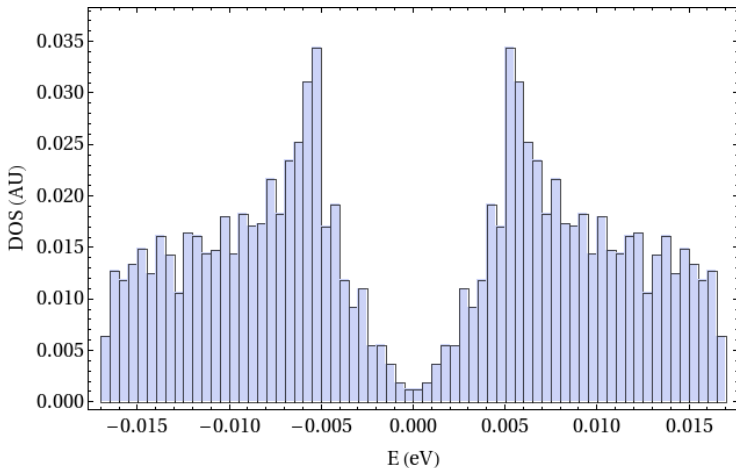
Each Landau Level becomes a set of $2p$ (tight-binding) bands with $\epsilon_{n,r}(k_1, k_2)$ for commensurate flux, $\phi / \phi_s = p/q$.

Results



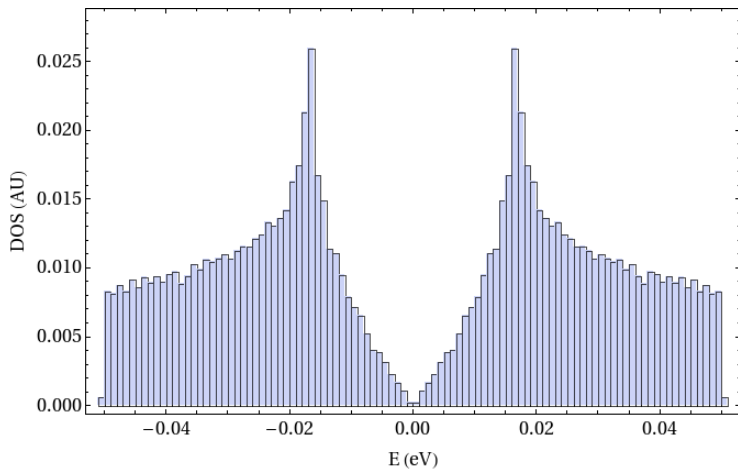
$$n = 0; p/q = 1/10; \quad L = 77 \overset{o}{\text{\AA}}; B \approx 8 T; \hbar\omega_c = 100 \text{ meV};$$

Results

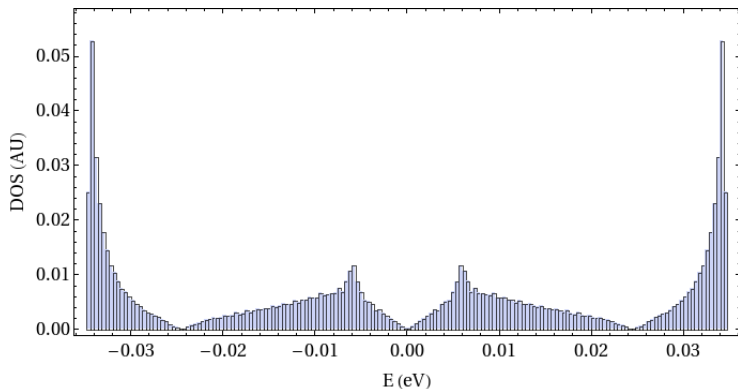


$n = 2$; $p/q = 1/10$; $L = 77 \overset{\circ}{\text{A}}$; $B \approx 8 T$; $\hbar\omega_c = 100 \text{ meV}$;

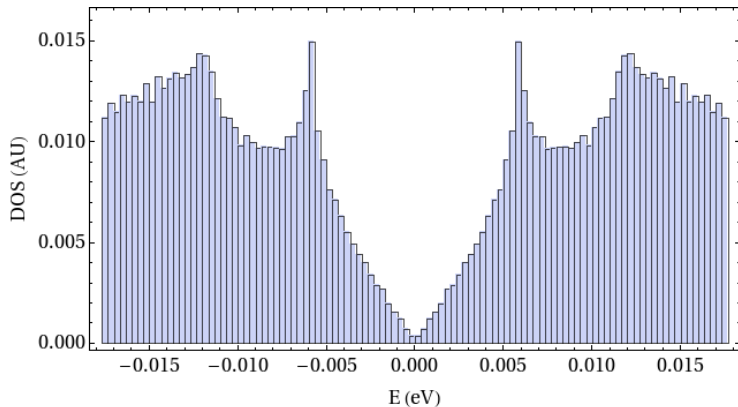
Results



$n = 1$; $p/q = 1/4$; $L = 77 \text{ \AA}$; $B \approx 19 \text{ T}$; $\hbar\omega_c = 150 \text{ meV}$;



$$n = 1; p/q = 2/9; \quad L = 77 \overset{o}{\text{\AA}}; B \approx 19 T; \hbar\omega_c = 150 \text{ meV};$$



$n = 0$; $p/q = 3/11$; $L = 77 \text{ \AA}$; $B \approx 19 \text{ T}$; $\hbar\omega_c = 150 \text{ meV}$;

Acknowledgements

Collaborators Nuno Peres, Antonio Castro Neto.

Rutgers Group Eva Andrei, Guohong Li, A. Luican.

Discussions Paco Guinea, Vitor Pereira, Eduardo Castro, Joanna Hass, Ed Conrad, Claire Berger.

Sponsors



UNIÃO EUROPEIA

Fundo Social Europeu

Condensed Matter Theory visitor's program

